GPS Solut (2014) 18:163–175
DOI 10.1007/s10291-014-0368-6

EDITORIAL

Performance evaluation of MSK and OFDM modulations for future GNSS signals

Xiaoli Liu · Muqing Liang · Yu Morton · Pau Closas · Ting Zhang · Zhigang Hong

Received: 4 July 2013 / Accepted: 28 January 2014 / Published online: 11 February 2014

Abstract The objective of this work is to investigate the performances of orthogonal frequency division multiplexing (OFDM) and minimum frequency shift keying (MSK) modulations as potential future global navigation satellite systems (GNSS) signal modulation schemes. MSK is used in global system for mobile communications because of its spectral efficiency, while OFDM is used in WLAN and digital video broadcast-terrestrial because of its multipath mitigation capability. These advantages of MSK and OFDM modulations render them as promising modulation candidates for future GNSS signals to offer enhanced performances in challenging environments. Gabor bandwidth and multipath error envelopes of these two modulations were computed and compared with those of the current global positioning system (GPS), Galileo, and Beidou signal modulations. The results show that OFDM modulation demonstrated promises as a viable future GNSS modulation, especially for signals that require pre-filtering bandwidths larger than 2 MHz, while MSK modulation is more desirable for pre-filtering bandwidth below 2 MHz where it exhibits the largest Gabor bandwidth.

Keywords GNSS · MSK · OFDM · Tracking performance · Multipath effects

X. Liu (✉) · M. Liang
School of Electrical Engineering, Wuhan University, Wuhan, China
e-mail: xlliu@whu.edu.cn

X. Liu · T. Zhang
GNSS Center, Wuhan University, Wuhan, China

Y. Morton
Electrical and Computer Department, Miami University, Oxford, OH, USA

P. Closas
Centre Tecnològic deTelecomunicacions de Catalunya, Barcelona, Spain

Z. Hong
China Academy of Surveying and Mapping, Beijing, China

Introduction

Binary phase shift keying (BPSK) modulation is the legacy modulation scheme used in satellite navigation signals such as the global positioning system (GPS). It is also widely used in communication systems despite its relatively low spectral efficiency. With the recent modernization of GPS and GLONASS signals and the emerging Beidou and Galileo systems, the number of navigation satellite signals in space is drastically increasing. Together with various regional navigation satellite systems and space-based augmentation systems, there will be more than 160 satellites and over 400 signals in space by the year 2030 (Betz 2013). Such a large number of signals will further exacerbate an already crowded radio spectrum and negatively impact the performance of all navigation systems sharing the limited resources. Therefore, improving the signal spectral efficiency to minimize mutual interference is a critical issue in future GNSS signal design.

A second issue in GNSS signal design is the multipath performance and interference mitigation ability (Hein et al. 2001). In modern satellite navigation systems, binary offset carrier (BOC) modulation has been used to address this issue. BOC signals occupy a wider spectrum and its autocorrelation function (ACF) shape has a sharper peak than that of BPSK (Betz 2001; Julien et al. 2004; Fantino et al. 2008; Zhang and Lohan 2011; Navarro-Gallardo et al. 2012). However, BOC modulations use square-wave

subcarriers, which have larger spectral side lobes and are more prone to produce larger interferences with signals of other coexisting navigation systems (Julien et al. 2004; Navarro-Gallardo et al. 2012).

To overcome the previously mentioned shortcomings, we investigate two alternative signal modulation schemes, the minimum frequency shift keying (MSK) and the orthogonal frequency division multiplexing (OFDM) techniques, as potential future satellite navigation signals. Both MSK and OFDM modulations are mature techniques with features such as constant envelope, compact spectrum, and good multipath-induced error performance. MSK offers better spectral confinement with lower side lobes compared to legacy satellite navigation signals. Previous studies show that the MSK signal offers comparable ranging accuracy to that of the BPSK signal for receivers with bandwidths of 2–4 MHz, which are typically used for GNSS signals (Hu et al. 2010; Ipatov and Shebshaevich 2011). MSK has already been utilized in a number of applications, such as mobile communications, micro-satellite communications, positioning and navigation systems, hybrid optical/wireless communication systems, deep space communications, and in the Blue Ray disc technology (Pasupathy 1979; Simon 2001). For example, the global system for mobile communications (GSM) uses a Gaussian-filtered MSK (GMSK) modulation. The ultra-wide band (UWB) multi-tag development platform, which is a UWB-based positioning system, implements a 2.4-GHz MSK ZigBee-like signal structure (Kuhn 2012). Ávila-Rodríguez et al. (2008a) suggested that existing GNSS signals could benefit by augmentation of MSK signals in the C band (4–8 GHz). For an exhaustive and systematic analysis of current as well as planned navigation signals, we refer the reader to the work in Ávila-Rodríguez (2008b) which provides a comprehensive treatment.

Orthogonal frequency division multiplexing modulation has also been widely used in mobile communication for the last decade (Cimini 1985; Zou and Wu 1995; Liu and Li 2004; Li et al. 2007). For example, the European digital video broadcast-terrestrial (DVB-T) system uses OFDM in the air interface. The OFDM-based DVB-T signal is currently a signal-of-opportunity candidate to provide coarse estimation of user positions when GNSS is not available or to assist GNSS in challenging environments (Serant et al. 2010; 2012). Applications of OFDM in wireless communication systems have demonstrated that it can provide reliable services for telecommunication and location-based systems with limited bandwidth. OFDM modulation has also been adopted by satellite communication systems (Kelley and Rigal 2007; ETSI EN 302 2008). Recent studies show that OFDM has a very efficient spectrum utilization rate and can provide accurate ranging performance (Thevenon et al. 2009; Mensing and Dammann 2008; Garmatyuk et al. 2011). With its high out-of-band attenuation property, OFDM modulation could be used as a new navigation signal and enable integrated communication and navigation services.

We compare performances of MSK and OFDM modulation with that of current GNSS signals, such as BPSK, BOC, and MBOC, by examining their time-domain models, power spectral densities, tracking accuracies, and multipath performances. Both theoretical and computer simulation-based results are shown. Theoretical modeling of tracking performance is presented in terms of ACF, Gabor bandwidth, and multipath error envelopes. Simulations showed that the OFDM multipath error envelope is smaller than that of other signals if the pre-filtering bandwidth is larger than 2 MHz, whereas MSK modulation is a competitive scheme for relatively low pre-filtering bandwidths. OFDM, however, has issues with the peak to average power ratio and is more vulnerable to synchronization errors (Proakis 2008).

We first present the mathematical models of the time-domain ACF and the power spectral density (PSD) of the modulations under study, and analyze the spectral separation coefficient of the different signals. Then, we compare the tracking performance of conventional correlation-based schemes in terms of Gabor bandwidth of the various modulations and their multipath error envelopes with multiple deterministic reflective signals. This is followed by evaluating the performance of a realistic channel models in which statistical models are used to generate parameters of multipath rays, and the conclusions.

Navigation signal properties of MSK and OFDM modulations

A good candidate navigation signal must possess several important characteristics. First, the signal ACF should have a narrow peak to allow precise range measurement. Second, a multipath signal should span a relatively small bias envelop in its range error profile, and thus limit the extent of potential multipath errors. Finally, efficient spectral utilization, or narrow PSD profiles are desirable to allow co-existence of a large number of signals with minimal mutual interference. In this section, these characteristics are analyzed for MSK, OFDM, and legacy GNSS modulations. For the sake of clarity, we provide a brief summary of fundamentals of each modulation.

Signal models

Minimum frequency shift keying is a continuous phase (CP) frequency shift keying (FSK) signal. The CP modulation family is particularly well suited for system

implementations that use nonlinear amplifiers (Proakis 2008; Pasupathy 1979). FSK is the digital version of the analog frequency modulation (FM). MSK is a special case of FSK with the modulation index set to 0.5. It has the minimum frequency separation that guarantees orthogonality among the modulation frequencies. Thus, non-coherent detection of MSK signals by discriminator detection, for instance, could provide low-cost and flexible implementations in some applications (Proakis 2008; Gronemeyer and Mcbride 1976).

Figure 1 shows the modulation scheme of a generic MSK signal. According to the principle of MSK modulation (Proakis 2008), the time-domain representation of the bandpass MSK modulation can be written as:

$$S_{\mathrm{MSK}}(t) = A\left(d(t)\sum_{m=1}^{\infty} a_m \cos(\pi(t-mT_{\mathrm{s}})/T_{\mathrm{s}})\Pi(t-mT_{\mathrm{s}})\right)\cos\omega_c t + A\left(\sum_{n=1}^{\infty} b_n \sin(\pi(t-nT_{\mathrm{s}}-T_{\mathrm{s}}/2)/T_{\mathrm{s}})\Pi(t-nT_{\mathrm{s}}-T_{\mathrm{s}}/2)\right)\sin\omega_c t \quad (1)$$

where

$$\Pi(t) = \begin{cases} 1 & 0 \le t \le T_{\mathrm{s}} \\ 0 & \text{otherwise} \end{cases} \quad (2)$$

is the shaping pulse, A is the complex amplitude of the signal, $d(t)$ is navigation data, a_m and b_n are binary codes, $\omega_c = 2\pi f_c$ is the angular carrier frequency, and $T_s = 1/f_s$ is the symbol length of the transmitted signal.

An OFDM signal splits a high-rate data stream into N complex parallel lower rate streams transmitted simultaneously over N orthogonal narrowband subcarriers, each carries one symbol (Serant et al. 2010; Thevenon et al. 2009; Proakis 2008; Diez et al. 2010). Figure 2 describes the OFDM modulation. The width of a subcarrier is narrow enough that the channel frequency response can be considered flat over the subcarrier bandwidth. The orthogonality among the subcarriers allows their spectra to overlap without mutual interference. Additionally, it can mitigate multipath effects because selective frequency fading at different subcarriers may result in an overall reduced multipath contribution to the receiver input.

The time-domain representation of the bandpass OFDM modulation is given by:

$$S_{\mathrm{OFDM}}(t) = Re\left\{\sum_{k=0}^{N-1} d_k a_k \cdot \Pi(t - T_s/2)\cdot \exp\left[j2\pi\left(f_0 + \frac{k}{T_s}\cdot \Delta f\right)t\right]\right\}\cos(\omega_c t). \quad (3)$$

where the index k refers to the k-th subcarrier, d_k is the data information transmitted at the k-th subcarrier, a_k is the binary code, N is the number of subcarriers, f_0 is the frequency of the first subcarrier carrier, Δf is the frequency interval between two adjacent subcarriers, and $f_0 + \frac{k}{T_s}\cdot\Delta f$ is the k-th subcarrier frequency.

PSD and ACF

The normalized PSD for an MSK signal is given by:

$$G_{\mathrm{MSK}}(f) = f_{\mathrm{s}}|S_{\mathrm{MSK}}(f)|^2 = \frac{8f_{\mathrm{s}}^3\cos^2\left(\frac{\pi f}{f_{\mathrm{s}}}\right)}{\pi^2\left(f_{\mathrm{s}}^2 - 4f^2\right)^2} \quad (4)$$

as represented by the signal model described in (1).

For an OFDM signal, we assume that the data bits modulating the subcarriers in each symbol period are statistically independent from each other and from that in previous or subsequent symbol periods (Scott and Farhang-Boroujeny 2008). As a result, the power spectrum of the overall signal can be expressed as the sum of the power spectra of the N individual subcarriers for any symbol period. Thus, the normalized power spectral density of an OFDM signal is given by:

$$G_{\mathrm{OFDM}}(f) = \frac{1}{N}\sum_{k=0}^{N-1} T_{\mathrm{s}}\left|\sigma_x^2\frac{\sin[\pi(f-f_k)T_{\mathrm{s}}]}{\pi(f-f_k)T_{\mathrm{s}}}\right|^2 \quad (5)$$

where, $\sigma_x^2 = \frac{1}{2}E\left[|a_k d_k|^2\right]$, f_k is the k-th subcarrier frequency. According to the Wiener–Khintchine theorem,

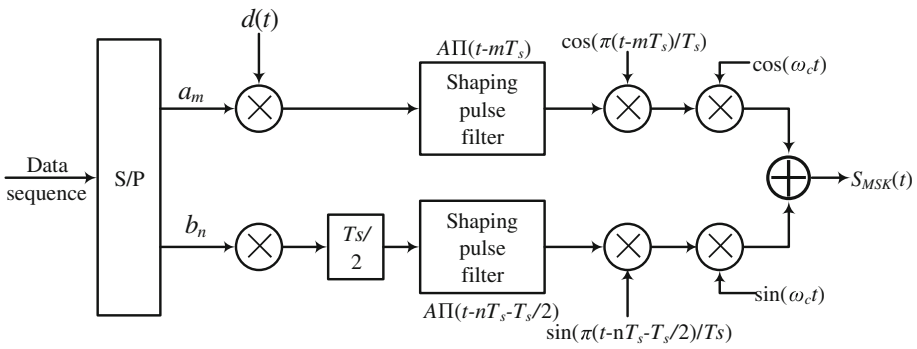

Fig. 1 MSK modulation schematic block diagram

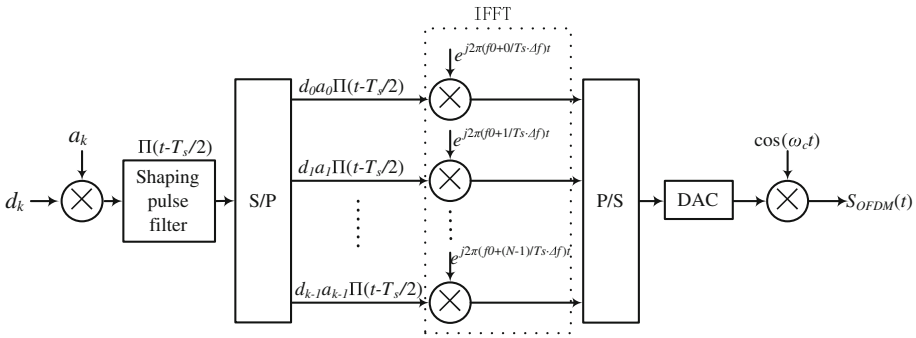

Fig. 2 OFDM modulation schematic block diagram

the ACF of a signal is the inverse Fourier transform of its corresponding PSD. Therefore, the ACFs for MSK and OFDM are:

$$R_{\mathrm{MSK}}(t) = \int_{-B_r/2}^{B_r/2} \frac{8f_s^3 \cos^2\left(\frac{\pi f}{f_s}\right)}{\pi^2\left(f_s^2 - 4f^2\right)^2} e^{j2\pi ft} df \tag{6}$$

$$R_{\mathrm{OFDM}}(t) = \int_{-B_r/2}^{B_r/2} \frac{1}{N}\sum_{n=1}^{N} T_s \left|\sigma_x^2 \frac{\sin[\pi(f-f_n)T_s]}{\pi(f-f_n)T_s}\right|^2 e^{j2\pi ft} df \tag{7}$$

respectively. B_r denotes the bandwidth of the corresponding signals defined by their PSDs. B_r may also be regarded as the pre-filtering bandwidth for GNSS receivers.

ACF and PSD simulation

We use simulation results to illustrate the spectrum efficiency and adjacent channel interference (ACI) suppression properties of MSK and OFDM modulations based on the ACF and PSD expressions described in the above subsection.

Figure 3 shows the PSD for MSK, OFDM, and several BPSK, BOC, and MBOD signals. BPSK(1), BPSK(2), and BPSK(10) are modulations used in GPS L1 CA, Beidou B1, and GPS L5 signals, respectively, while BOC(1,1) and MBOC(6,1,1/11) are used in Galileo E1 signal. The code rates are 10.23 Mcps for BPSK(10), 2.046 Mcps for BPSK(2), and 1.023 Mcps for the remaining signals. The number of subcarriers in the OFDM modulation is 64.

Minimum frequency shift keying modulation is a constant envelop signal with phase continuity during bit transitions. The phase continuity makes the PSD compact, falling off rapidly with increasing frequency as shown in Fig. 3. This property makes MSK a spectrum efficient modulation scheme compared to other signals. Moreover, it can be seen from Fig. 3 that the main lobe of an MSK signal is larger than that of a BPSK and OFDM signals, implying that most of the energy of MSK modulation is concentrated within the main lobe, while the side lobes

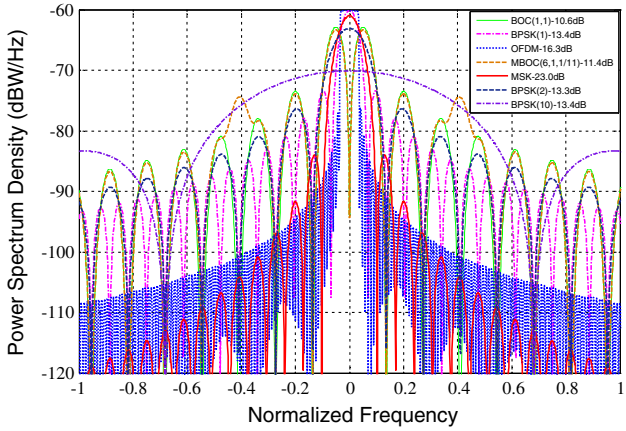

Fig. 3 Comparison of PSDs for MSK, OFDM, BPSK, BOC, and MBOC modulations. The relative power attenuations between the first side lobe and the main lobe (in dB) are also listed in the figure

magnitude decreases rapidly. Therefore, it is less vulnerable to ACI caused by other closely spaced signal sources in the frequency domain.

Figure 3 also shows that the side lobes of MSK, OFDM, BPSK(1), BPSK(10), BPSK(2), BOC (1,1), and MBOC (6,1,1/11) are about 23, 16.3, 13.4, 13.4, 13.3, 10.6, and 11.4 dB lower than their corresponding main lobes, respectively. Therefore, both the MSK and OFDM modulations have superior spectrum efficiency compared with the other legacy modulations shown in the figures.

Figure 4a–c shows the ACF for several above modulation schemes with 2, 4, and 20 MHz pre-filtering bandwidths, respectively. For the 2 MHz pre-filtering bandwidth, the MSK outperforms the BPSK signal because the total power within 2 MHz for MSK is larger than that of the BPSK. For such a narrow pre-filtering bandwidth, MBOC appears to have the most advantage, followed by OFDM. As the pre-filtering bandwidth increases, the MSK modulation performance deteriorates while the OFDM ACF became increasingly steep. When the pre-filtering bandwidth is 20 MHz, which is much larger than the main lobe bandwidth of the BPSK modulation signal, the OFDM presents superior tracking performance with the narrowest ACF among the signals analyzed.

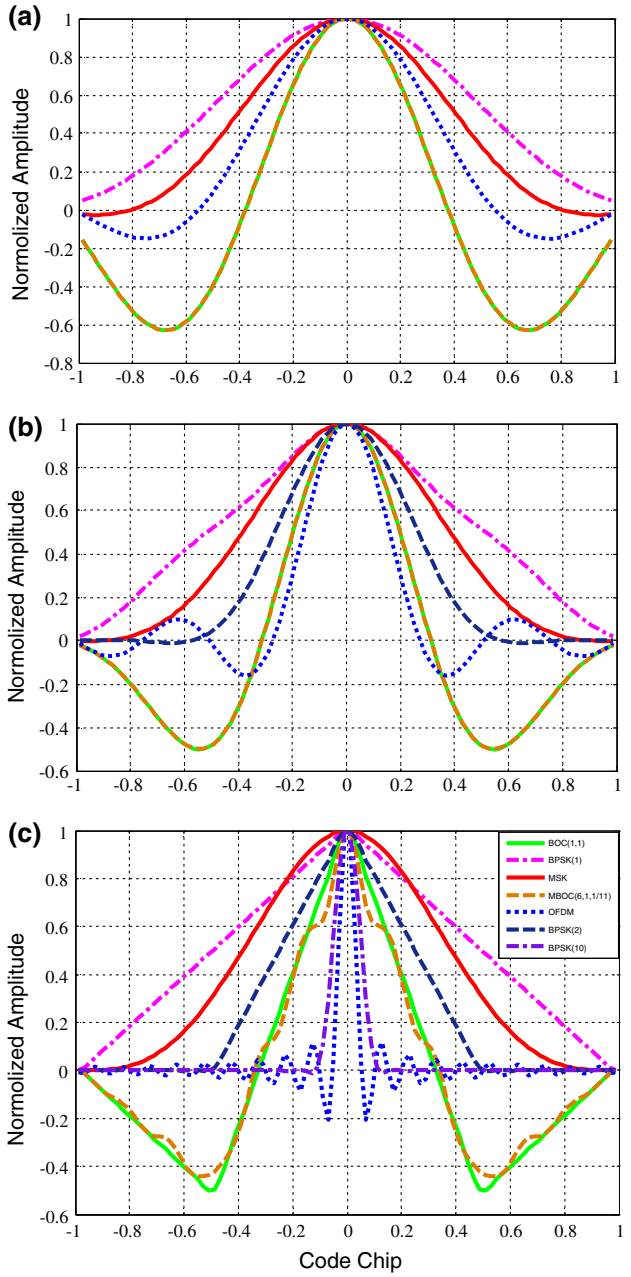

Fig. 4 ACF for MSK, OFDM, BPSK, BOC, and MBOC modulated signals with **a** 2 MHz, **b** 4 MHz and **c** 20 MHz pre-filtering bandwidths

Interference mitigation properties

Mutual interference and compatibility among GNSS signals are fundamental measures of navigation signal performance (Wallner et al. 2005). The spectral separation coefficient (SSC) is a conventionally used mean to quantify these characteristics (Betz and Goldstein 2002). The SSC measures the amount of interference imposed on a signal from other GNSS signals sharing the same frequency band. Two SSC parameters are typically defined as the following:

$$k_{\mathrm{dd}} = \int_{-\infty}^{\infty} G_{\mathrm{d}}^2(f)df \tag{8}$$

$$k_{\mathrm{id}} = \int_{-\infty}^{\infty} G_{\mathrm{i}}(f)G_{\mathrm{d}}(f)df \tag{9}$$

where $G_{\mathrm{d}}(f)$ and $G_{\mathrm{i}}(f)$ are the normalized power spectral densities of the desired and interfering signals, respectively. Clearly, k_{dd} quantifies a signal's self-imposed SSC, and k_{id} defines the SSC between a desired and interfering signals.

The SSCs for the modulations presented in this paper are shown in Table 1. Table 2 lists the pseudo codes used to compute the SSC values. The pre-filtering bandwidth used in the calculation is 20 MHz. The color-coded cells provide a quick view of the performances of the modulations schemes under investigation. Clearly, the OFDM modulation offer the smallest SSCs, followed by BPSK(10), MBOC(6,1,1/11), BOC(1,1), BPSK(2), MSK, and BPSK(1). This is not surprising because OFDM signals consist of overlapping and mutually orthogonal subcarriers, resulting in very efficient spectrum utilization (Bingham 1990). Therefore, the inter-carrier interference (ICI) of OFDM signal can be largely mitigated, assuming small subcarrier synchronization errors. The SSCs values of the MSK modulation are almost 10 dB higher than those of OFDM signals. The highest SSCs values are associated with MSK and BPSK modulations.

Tracking performance

This section presents tracking performance of the modulation schemes based on analysis of their Gabor bandwidths and multipath error envelopes. The conventional two-ray multipath model is extended to three and four rays to provide more extensive multipath bias error analysis.

Gabor bandwidth

The generic approach to evaluate the theoretical accuracy of time-delay estimation is based on the Gabor bandwidth defined as the root of the second moment of the power spectral density of a signal (Gabor 1946; Ávila-Rodríguez et al. 2006):

$$\Delta f_{\mathrm{Gabor}} = \sqrt{\int_{-B_{\mathrm{r}}/2}^{B_{\mathrm{r}}/2} f^2 G(f)df} \tag{10}$$

where, $G(f)$ is the normalized PSD of the signal. The Gabor bandwidth can be seen as an alternative interpretation of a

Table 1 SSC values for BPSK, BOC, MBOC, MSK, and OFDM for 20 MHz pre-filtering bandwidth

SSCs (dB)	BPSK(1)	MSK	BPSK(2)	BOC(1,1)	MBOC(6,1,1/11)	BPSK(10)	OFDM
BPSK(1)	-61.9	-62.3	-63.9	-67.9	-68.3	-70.2	-75.6
MSK	-62.3	-62.4	-63.8	-66.3	-66.7	-70.1	-75.5
BPSK(2)	-63.9	-63.8	-64.9	-66.1	-66.5	-70.4	-75.7
BOC(1,1)	-67.9	-66.3	-66.1	-65	-65.3	-70.6	-75.8
MBOC(6,1,1/11)	-68.3	-66.7	-66.5	-65.3	-65.7	-70.9	-75.9
BPSK(10)	-70.2	-70.1	-70.4	-70.6	-70.9	-71.9	-76.3
OFDM	-75.6	-75.5	-75.7	-75.9	-76	-76.4	-76.4
75-80 dB		70-75 dB		65-70 dB		60-65 dB	

Table 2 Pseudo code for SSC calculation

1: Initialize settings, *Rc*, B_r, *N*, N_{bins}, where *Rc* is the code rate, B_r is the pre-filtering bandwidth of the receiver, *N* is the number of subcarriers, and N_{bins} the number of bins for numerical integration.

2: Generate N_{bins} equally spaced frequency bins, f_i, in $[-B_r/2, B_r/2]$

3: **for** $i = 1$–2

4: **for** $j = 1$–2

5: Compute $G_i(f_i)^* G_j(f_i)$ for each bin f_i, where $G_i(f)$ and $G_j(f)$ are the PSDs described in (4) and (5),respectively,

6: Compute k_{dd} or k_{id}, by addition of $G_i(f_i)^*G_j(f_i)$ over all evaluated frequency bins.

7: **end for** j

8: **end for** i

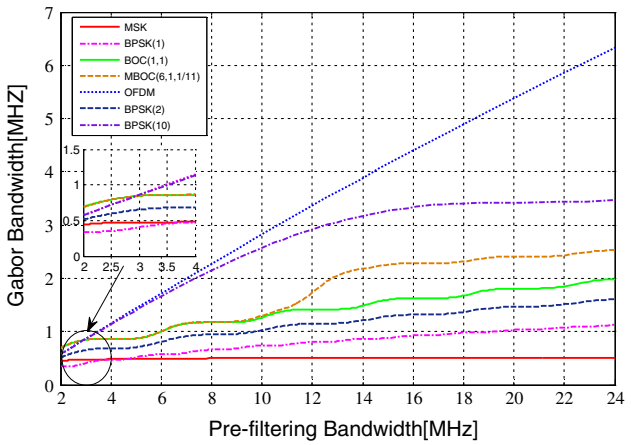

Fig. 5 Gabor bandwidth as a function of the pre-filtering bandwidth

signal's Cramér–Rao lower bound. Therefore, the greater the Gabor bandwidth, the better the code-tracking accuracy will be.

Substituting the PSDs of different modulations under consideration into (10), we computed the Gabor bandwidth for a front-end bandwidth ranging from 2 to 24 MHz. The results are shown in Fig. 5.

Figure 5 shows that when the front-end bandwidth is <4 MHz, the Gabor bandwidth of MSK is higher than that of the BPSK. This indicates that the code-tracking performance of MSK signals is better than that of BPSK for pre-filtering bandwidths below 4 MHz. The MSK Gabor bandwidth appears to have reached its peak value at around 4 MHz, while for other modulations shown in Fig. 5, their Gabor bandwidth continues to increase as the pre-filtering bandwidth increases. The Gabor bandwidth of the OFDM is the largest if the pre-filtering bandwidth is above 4 MHz. Therefore, the OFDM shows the best code-tracking performance among the analyzed signals for large pre-filtering bandwidths.

Multipath error envelope

The multipath error envelope based on a two-ray signal model is a classic figure of merit in describing the multipath performance of a signal. It quantifies the multipath-induced bias as a function of the relative delays between rays. The carrier phase difference, code delay difference, and signal power ratio between a multipath signal and its direct line of sight (DLOS) signal are all important quantities that directly impact the tracking loop errors (Van Dierendonck et al. 1992).

In a two-ray model, the estimation of the DLOS signal delay time, which is an approximation of the ACF derivative, can be obtained from the zero-crossing of the S curve (Braasch 1996):

$$\begin{aligned} D(\varepsilon) = {} & [R(\varepsilon + d/2) - R(\varepsilon - d/2)] \\ & + a[R(\varepsilon - \Delta\tau_1 + d/2) - R(\varepsilon - \Delta\tau_1 - d/2)] \\ & \times \cos(\Delta\phi_1) \equiv 0 \end{aligned} \tag{11}$$

where a is the multipath to direct signal amplitude ratio (MDR), $\Delta\phi_1$ is carrier phase difference between the multipath and the DLOS, ε is the delay estimation error, and d is the correlator time spacing between the early and late reference signals.

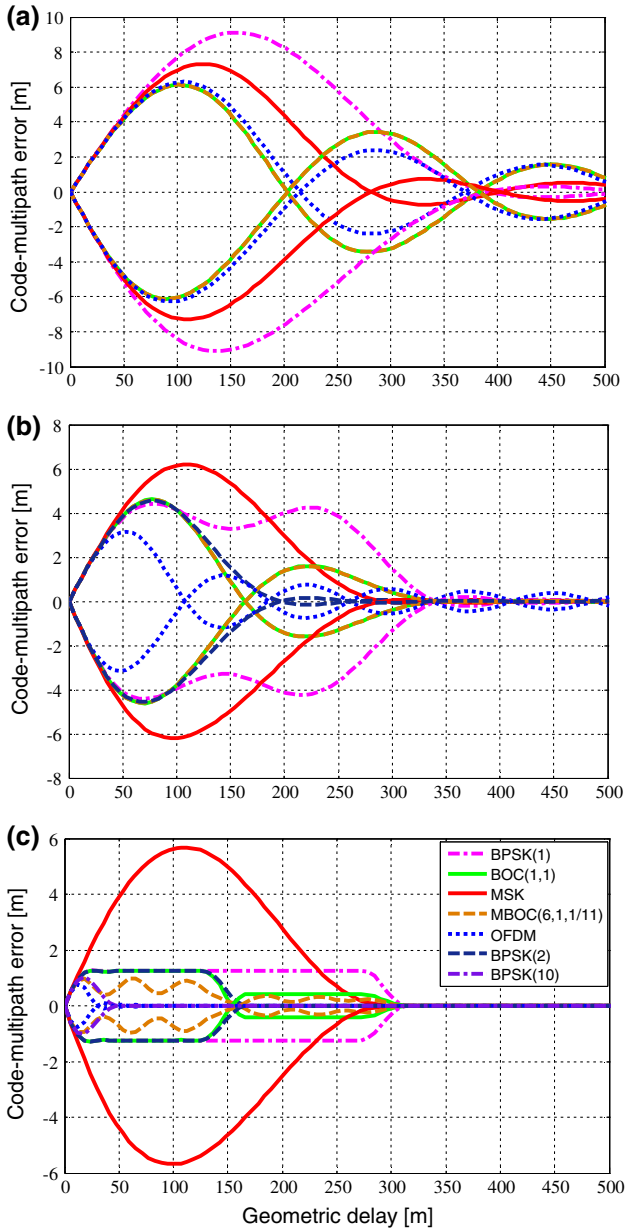

Fig. 6 Multipath error envelopes of pre-filtering bandwidth of 2 MHz (**a**), 4 MHz (**b**) and 20 MHz (**c**), $a = 0.1$, $d = 0.1$ chip

The cases where $\Delta\phi_1 = 0$ and π correspond to the worse possible multipath-induced bias (Van Nee 1993), and thus the multipath error envelopes are computed using these two extreme cases. Linear approximation of $D(\varepsilon)$ around $\varepsilon = 0$ is typically used to simplify analysis (He et al. 2011):

$$D(\varepsilon) = D(0) + D'(0) \times \varepsilon + o\left(\varepsilon^2\right). \tag{12}$$

The last term in (12) corresponds to higher-order errors. Neglecting the higher-order error leads to:

$$\varepsilon \approx -D(0)/D'(0). \tag{13}$$

Table 3 Two-ray model multipath error calculation test cases

Modulation situation	MSK/OFDM
Varying a	Figure 7
$a = 0.1, 0.25, 0.5$	
$d = 0.1$ chip	
Code rate = 1.023 Mcps	
Pre-filtering BW = 2 MHz	
Varying code rate	Figure 8
$a = 0.1$	
$d = 0.1$ chip	
Code rate = 1.023, 2.046, 10.23, 20.46 Mcps	
Pre-filtering BW = 40 MHz	
Varying d	Figure 9
$a = 0.1$	
$d = 0.1, 0.5, 1$ chip	
Code rate = 1.023 Mcps	
Pre-filtering BW = 2 MHz	

The signal ACF is given as:

$$R(\tau) = \int_{-B_r/2}^{B_r/2} G(f)\, e^{j2\pi f\tau} df. \tag{14}$$

The multipath error envelope of a signal can be approximated based on (11), (13), and (14):

$$\varepsilon \approx \frac{\pm a \int_{-B_r/2}^{B_r/2} G(f)\sin(2\pi f\tau)\sin(\pi f d)df}{2\pi \int_{-B_r/2}^{B_r/2} fG(f)\sin(\pi f d)[1 \pm a\cos(2\pi f\tau)]df}. \tag{15}$$

In the Eq. 15, "+" and "−" correspond to when the phase difference between the multipath and the DLOS signal is equal to 0 and π.

We computed the multipath envelope for correlator spacing $d = 0.1$ chip and MDR $a = 0.1$. Figure 6a–c shows the multipath error envelopes for 2, 4, and 20 MHz pre-filtering bandwidths, respectively. Note that for BPSK(10), we only computed the envelope for a 20-MHz pre-filtering bandwidth, as the 2 and 4 MHz values are below the signal Nyquist frequency. Similarly, for BPSK(2) modulation, only pre-filtering bandwidths of 4 and 20 MHz are used in the calculation.

For the 2 MHz pre-filtering bandwidth, the multipath error of MSK modulation was smaller than that of the BPSK signal. When the pre-filtering bandwidth is 4 and 20 MHz, the OFDM exhibits a much smaller multipath-induced error compared with all other modulations investigated. At 20 MHz bandwidth, both OFDM and BPSK(10) have a small multipath envelop of below 1 m, and the OFDM envelop is barely visible when the multipath delay is larger than 25 m. These results are in accord with the Gabor bandwidth analysis performed earlier. At 4 MHz

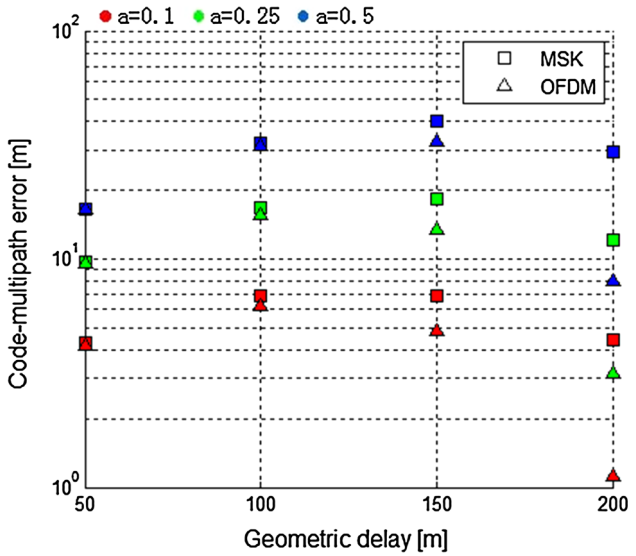

Fig. 7 Multipath error for MSK and OFDM with different MDR values

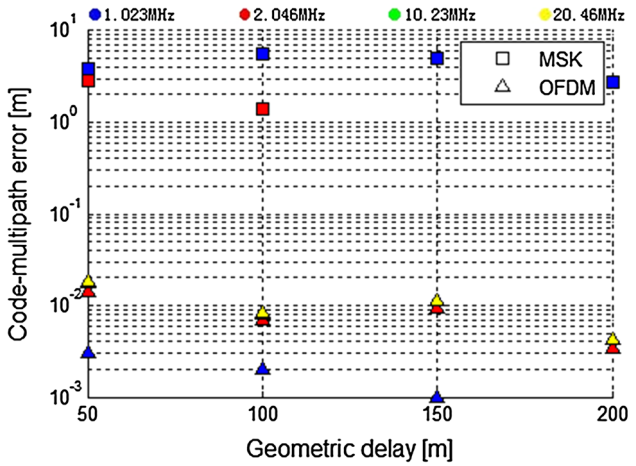

Fig. 8 Multipath error for MSK and OFDM with different code rate values

bandwidth, BPSK(2) presents the smallest multipath envelop when the delay is over 200 m.

We further compared multipath-induced errors for MSK and OFDM based on the two-ray model. Table 3 lists the test cases used in the comparison. The results are illustrated in Figs. 7, 8, and 9.

Figure 7 shows the case for a pre-filtering bandwidth of 2 MHz. Overall, for this small pre-filter bandwidth value, the multipath-induced errors of MSK and OFDM are on the same order of magnitude (below 40 m) for the range of a values used when the delay is <100 m. As the delay increases, the multi-path error for OFDM decreases much more rapidly compared with that of MSK.

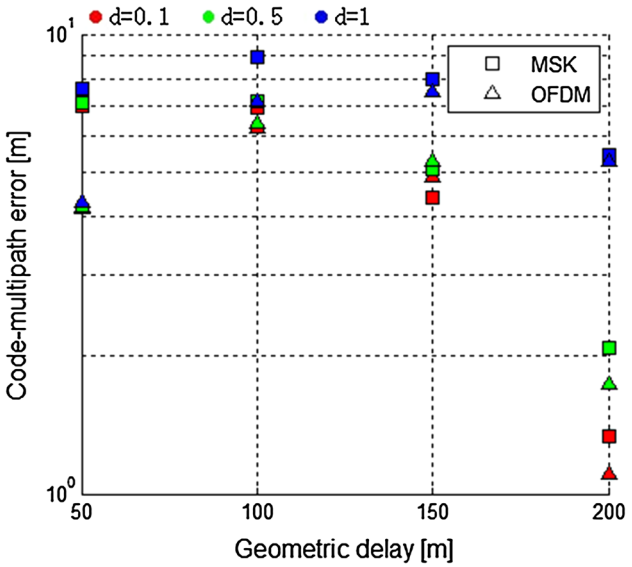

Fig. 9 Multipath error for MSK and OFDM with different correlator spacings

Figure 8 shows the multipath-induced errors with the different code rates. A large pre-filtering bandwidth of 40 MHz is used in the calculation. The multipath-induced error for the MSK signal decreases drastically as the code rate increases and approaches zero when the code rate is 10.23 or 20.46 Mcps (not shown in the figure). This result agrees with previous studies that a signal with a high code chip rate will have smaller multipath errors (Braasch 1996; Byun et al. 2002; Kaplan and Hegarty2006). Figure 8 shows that multipath-induced errors for OFDM signals are only in the cm level, nearly 100 times below that of MSK. Note that the code-multipath errors with OFDM rise slightly as the code rate increases, an effect observed in OFDM at high chip rates in a previous study (Neito 2006).

Figure 9 shows multipath errors are smaller for narrower correlator spacings. The impact of the correlator spacing is more prominent for larger delays. For small delays within 50 m, multipath error for MSK and OFDM signals is not very sensitive to correlator spacing. Additionally, the multipath error with different numbers of subcarrier was also simulated, and the results show that the multipath error envelope with OFDM modulation is not sensitive to the numbers of subcarrier as it mainly depends on the parameters characterizing each subcarrier.

Multipath bias of multiple rays

We further expanded (15) to model three-ray and four-ray multipath study cases following the two-ray model approach. The analytical expressions of multipath-caused biases are:

$$\varepsilon_{3-\text{ray}} \approx \frac{\pm \int_{-B_r/2}^{B_r/2} G(f)[a_1 \sin(2\pi f\tau_1) + a_2 \sin(2\pi f\tau_2)] \sin(\pi fd) df}{2\pi \int_{-B_r/2}^{B_r/2} fG(f) \sin(\pi fd)[1 \pm a_1 \cos(2\pi f\tau_1) \pm a_2 \cos(2\pi f\tau_2)] df} \tag{16}$$

$$\varepsilon_{4-\text{ray}} \approx \frac{\pm \int_{-B_r/2}^{B_r/2} G(f)[a_1 \sin(2\pi f\tau_1) + a_2 \sin(2\pi f\tau_2) + a_3 \sin(2\pi f\tau_3)] \sin(\pi fd) df}{2\pi \int_{-B_r/2}^{B_r/2} fG(f) \sin(\pi fd)[1 \pm a_1 \cos(2\pi f\tau_1) \pm a_2 \cos(2\pi f\tau_2) \pm a_3 \cos(2\pi f\tau_3)] df} \tag{17}$$

where, a_i and τ_i are the amplitude and delay of the i-th multipath ray with respect to the DLOS signal. To assess the multipath performance in more realistic situations, Figs. 10 and 11 show the running average multipath error (Irsigler et al. 2005) with the three-ray model and the four-ray model, respectively. The MDR values are set to $a_1 = 0.3$, $a_2 = 0.2$, and $a_3 = 0.1$. The relative delays between the multipath rays and DLOS signal are $\tau_2 = \tau_1 + 0.1{*}T_s$ and $\tau_3 = \tau_1 + \tau_2 + 0.1{*}T_s$ chips, which are allowed to vary from 0 to 500 m. The top and bottom plots in each figure correspond to a pre-filtering bandwidth of 4 and 20 MHz, respectively. These biases are generally higher than that of the two-ray model. This is understandable as more rays will no doubt introduce additional multipath contributions. For short geometric delays such as <25 m for the three-ray case and 10 m for the four-ray case, all modulations under investigation show similar average multipath errors. As the geometric delay increases, the average multipath errors also diverge among the modulations with OFDM modulation showing superior multipath performance. For very large geometric delays, OFDM, BPSK(10), MBOC, BOC(1,1), and BPSK(2) all have similar performances.

Analysis under realistic channel models

An experimentally derived realistic satellite-to-user dynamic channel model is used to evaluate the modulation performance. The channel model is generated from a high-resolution measurement campaign carried out at the

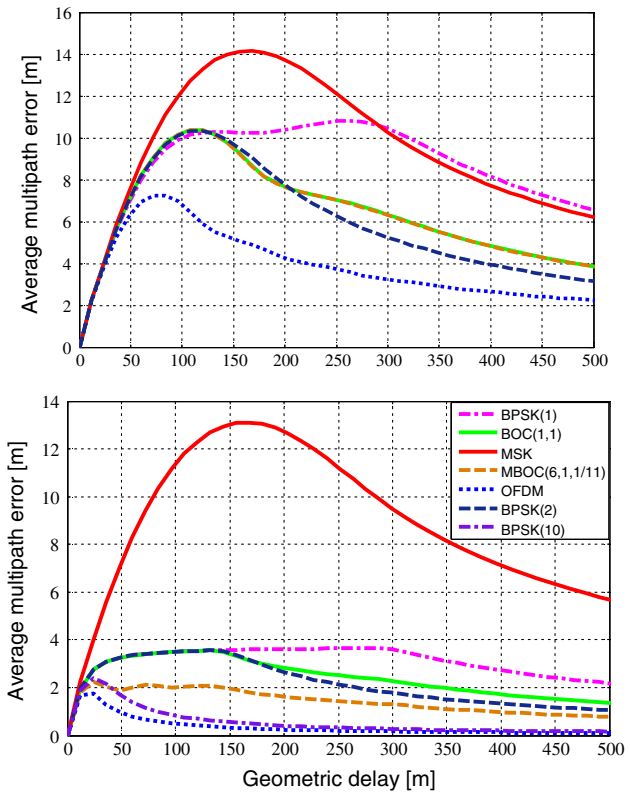

Fig. 10 Multipath-caused error for three-ray model with pre-filtering bandwidth of 4 MHz (*top*) and 20 MHz (*bottom*) for three-ray model

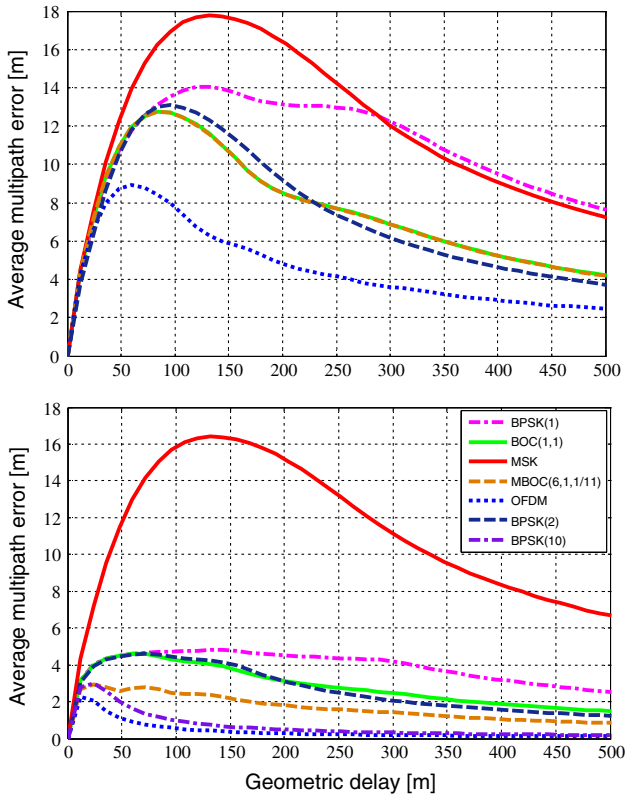

Fig. 11 Multipath-caused error for four-ray model with pre-filtering bandwidth of 4 MHz (*top*) and 20 MHz (*bottom*)

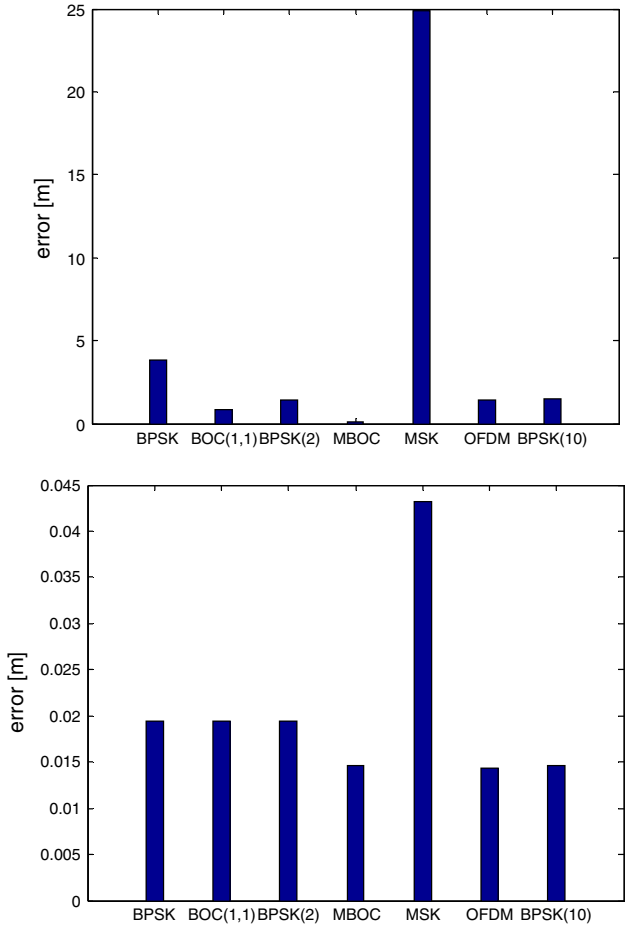

Fig. 12 Average multipath-caused bias in the realistic channel model for satellite elevation of 30° (*top*) and 80° (*bottom*)

German Aerospace Center (DLR) during 2002. Details of the campaign, data analysis, and the proposed land mobile channel can be found in Steingass and Lehner (2004) and Lehner and Steingass (2005). The model was recently standardized in ITU-R P.681-7 (10/09) "Propagation data required for the design of Earth-space land mobile telecommunication systems". The model, wherein the user platform moves, consists of obstacles such as houses, trees, and poles whose shape can be parameterized. The output of the model is a random set of multipath rays, with powers and delays that evolve with time.

We adopted a setup corresponding to a vehicle moving at a maximum speed of 50 km/h in a suburban environment, constituting a very challenging, multipath-rich environment. We considered two cases, one where the satellite had an elevation of 80° and another with 30°, with the latter being more prone to multipath. The situation is similar to that used in (Closas and Fernández-Prades 2011), and thus we refer the reader there to see the power delay profile of the simulated case.

The various modulations were tested using a realistic channel model with correlator spacing equal to 0.1 chips and a pre-filtering bandwidth at the receiver of 20 MHz. The results for the 30° and 80° elevations are shown in Fig. 12. The results show that the worst performance is given by the MSK modulation for both satellites. This is in accordance with the multipath error envelopes, the Gabor bandwidth, and the SSC analyses we performed earlier. While in general the channel characteristics of a satellite at an elevation of 80° are more benign than the one at 30°, the results also show that all other modulations have similar performance for the high elevation satellite, while the MBOC and BOC(1,1) modulation outperforms OFDM, BPSK(2), and BPSK(10) for the low elevation satellite.

Conclusions

Both MSK and OFDM modulations are often applied to satellite and mobile communication systems due to their superior performance compared with the traditional BPSK modulation in terms of larger out-of-band attenuation. Based on their mathematical expressions, we investigated the suitability of these modulations for navigation purposes. Besides the interference computations involving these investigated signals in the shared band, we analyzed the tracking performance of conventional correlation-based schemes for MSK and OFDM modulations in terms of the Gabor bandwidth and its multipath error envelopes when compared to current GPS, Galileo and Beidou signals. Both theoretical and computer simulation-based results are in agreement, showing that the tracking performance with OFDM modulation outperforms the other signals investigated. Furthermore, the multipath-induced error in OFDM signals is reduced by increasing the pre-filtering bandwidth or the code rate, whereas it is less sensitive to the correlator spacing variations. No difference was observed when additional subcarriers were used. On the other hand, multipath-induced errors in the MSK modulation are less than that of BPSK and similar to that of OFDM with a 2 MHz pre-filtering bandwidth. Our simulation results showed that increasing the code rate reduces the multipath error.

Realistic channel models in multipath-rich suburban environment were also used to evaluate the various modulations performances for pre-filtering bandwidth of 20 MHz. The results showed that MSK modulation has the largest errors while the MBOC has the least error for a low elevation satellite. The OFDM signal showed comparable performance with most of the remaining modulations.

Acknowledgments This work was supported by the contract of 201122, funded by Key Laboratory of Geo-Informatics of National Administration of Surveying, Mapping and Geoinformation of China. Additionally, this work has been partially supported by the Spanish Ministry of Economy and Competitiveness project TEC2012-39143 (SOSRAD) and by the European Commission in the framework of the FP7 Network of Excellence in Wireless COMmunications NEWCOM# (Grant agreement No. 318306). The Key Project of National Natural Science Foundation of China (No: 41231174) also supported this research. The authors appreciate the reviewers for their constructive comments and suggestions which have significantly improved the quality of this work.

References

Ávila-Rodríguez JA (2008b) On generalized signal waveforms for satellite navigation. Dissertation, University FAF Munich

Ávila-Rodríguez JA, Pany T, Hein GW (2006) Bounds on signal performance regarding multipath-estimating discriminators. Proceedings of ION-GNSS-2006, Institute of Navigation, Fort Worth, TX, pp 1710–1722

Ávila-Rodríguez JA, Wallner S, Won JH, Eissfeller B, Schmitz-Peiffer A, Floch JJ, Colzi E, Gerner JL (2008a) Study on a Galileo signal and service plan for C-band. Proceedings of ION-GNSS-2008, Institute of Navigation, Savannah, GA, pp 2515–2529

Betz JW (2001) Binary offset carrier modulations for radionavigation. Navigation 48(4):227–246

Betz JW (2013) Signal structures for satellite-based navigation: past, present, and future. Proceedings of ION-Pacific PNT-2013, Institute of Navigation, Honolulu, HI, pp 131–137

Betz JW, Goldstein DB (2002) Candidate designs for an additional civil signal in GPS spectral bands. Proceedings of ION-GNSS-2002, San Diego, CA, pp 622–631

Bingham JAC (1990) Multi-carrier modulation for data transmission: an idea whose time has come. IEEE Commun Mag 28(5):5–14. doi:10.1109/35.54342

Braasch MS (1996) Multipath effects. In: Parkinson B, Spilker J, Axelrad P, Enge P (eds) Global positioning system: theory and application, vol 1. American institute of aeronautics and astronautics, Inc: Washington, chapter 14, pp 547–568

Byun SH, Hajj GA, Young LE (2002) Assessment of GPS signal multipath interference. Proceedings of ION-GNSS-2002, Institute of Navigation, San Diego, CA, pp 694–705

Cimini LJ (1985) Analysis and simulation of a digital mobile channel using orthogonal frequency division multiplexing. IEEE Trans Commun 33(7):665–675. doi:10.1109/TCOM.1985.1096357

Closas P, Fernández-Prades C (2011) A statistical multipath detector for antenna array based GNSS receivers. IEEE Trans Wirel Commun 10(3):916–929

Diez J, De Castro D, Palomo JM, Tossaint M (2010) Integrated navigation and communication system based on OFDM. In: Proceedings of NAVITEC, Noordwijk, The Netherlands, 8–10 Dec pp 1–5. doi:10.1109/NAVITEC.2010.5707995

ETSI EN 302 583V1.1.1 (2008) Digital Video Broadcasting (DVB): Framing structure, channel coding and modulation for satellite services to handheld devices (SH) below 3 GHz. European standard (Telecommunications series). http://www.etsi.org/deliver/etsi_en/302500_302599/302583/01.01.01_60/en_302583v010101p.pdf. Accessed 26 Jan 2013

Fantino M, Marucco G, Mulassano P, Pini M (2008) Performance analysis of MBOC, AltBOC and BOC modulations in terms of multipath effects on the carrier tracking loop within GNSS receivers. In: Proceedings of IEEE/ION PLANS, Monterey, CA, pp 369–376. doi:10.1109/PLANS.2008.4570092

Gabor D (1946) Theory of communication. J Inst Electr Eng 93(3):429–457

Garmatyuk D, Morton Y, Mao XL (2011) Radar and GPS system inter-operability with UWB-OFDM signals. IEEE Trans Aerosp Electron Syst 47(1):265–274

Gronemeyer SA, Mcbride AL (1976) MSK and offset QPSK modulation. IEEE Trans Commun 24(8):809–820

He ZM, Hu YH, Wu JF, Wang JG, Hou J, Wang K (2011) A Comprehensive method for multipath performance analysis of GNSS navigation signals. In: Proceedings of ICSPCC, Shaanxi, China, 14–16 Sept, pp 1–6. doi:10.1109/ICSPCC.2011.6061564

Hein GW, Godet J, Issler JL, Martin JC, Lucas-Rodriguez R, Pratt T (2001) The Galileo frequency structure and signal design. Proceedings of ION-GNSS-2001, Institute of Navigation, Salt Lake City, UT, pp 1273–1282

Hu XL, Ran YH, Liu YQ (2010) New option for modulation in GNSS signal design. Syst Eng Electr 32(9):1962–1967 (in Chinese)

Ipatov VP, Shebshaevich BV (2011) Spectrum compact signals: a suitable option for future GNSS. Inside GNSS 6(1):47–53

Irsigler M, Avila-Rodriguez JA, Hein GW (2005) Criteria for GNSS multipath performance assessment. Proceedings of ION-GNSS-2005, Institute of Navigation, Long Beach, CA, pp 13–16

Julien O, Macabiau C, Cannon ME, Lachapelle G (2004) New unambiguous BOC(n,n) signal tracking technique. In: Proceedings of NAVITEC'2004, Noordwijk, The Netherlands, 8–10 Dec, p 8

Kaplan ED, Hegarty CJ (2006) Understanding GPS: principles and applications, 2nd edn. Artech house, London

Kelley P, Rigal C (2007) DVB-SH—mobile digital TV in S-band. Tech review 311 EBU Technical review, p 9. https://tech.ebu.ch/docs/techreview/trev_311-dvb_sh.pdf. Accessed 26 Jan 2013

Kuhn MJ (2012) Development and experimental analysis of wireless high accuracy ultra-wideband localization systems for indoor medical applications. Dissertations, University of Tennessee, pp 179–229

Lehner A, Steingass A (2005) A novel channel model for land mobile satellite navigation. Proceedings of ION-GNSS-2005. Institute of Navigation, Long Beach, CA, pp 2132–2138

Li B, Qin Y, Low C, Gwee C (2007) A survey on mobile WiMax. IEEE Commun Mag 45(12):70–75

Liu C, Li F (2004) Spectrum modelling of OFDM signals for WLAN. Electron Lett 40(22):1431–1432. doi:10.1049/el:20046524

Mensing C, Dammann A (2008) Positioning with OFDM based communications systems and GNSS in critical scenarios. In: Proceedings of WPNC'08, Hannover, Germany, March 27, p 7

Navarro-Gallardo M, Lopez-Risueno G, Crisci M, Seco-Granados G (2012) Analysis of side lobes cancellation methods for BOC-cos(n,m) signals. In: Proceedings of NAVITEC, Noordwijk, The Netherlands, 5–7 Dec, pp 1–7. doi:10.1109/NAVITEC.2012.6423115

Neito J (2006) Effects of code rate and channel estimation on OFDM and OFDM-CDMA waveforms. In: Rao RM, Dianat SA, Zoltowski MD (ed) Wireless sensing and processing. Proceedings of SPIE. Orlando, FL, 17 April, vol. 6248, pp 62480 K. doi:10.1117/12.665472

Pasupathy S (1979) Minimum shift keying: a spectrally efficient modulation. IEEE Commun Mag 17(4):14–22

Proakis JG (2008) Digital communications, 5th edn. McGraw-Hill, New York

Scott LT, Farhang-Boroujeny Behrouz (2008) Spectral method of blind carrier tracking for OFDM. IEEE Trans Signal Process 56(7):2706–2717

Serant D, Julien O, Macabiau C, Thevenon P, Corazza S, Dervin M (2010) Development and validation of an OFDM/DVB-T sensor for positioning. In: Proceedings of IEEE/ION PLANS, Indian Wells, CA, 4–6 May, pp 988–1001. doi:10.1109/PLANS.2010.5507273

Serant D, Julien O, Thevenon P, Ries L, Dervin M (2012) Testing OFDM-based positioning using the digital TV signals. In: Proceedings of EUSIPCO, Bucharest, 27–31 August, pp 539–543

Simon MK (2001) Bandwidth efficient digital modulation with application to deep space communications. In: Yuen Joseph H (ed) JPL deep-space communications and navigation series. Wiley, New York

Steingass A, Lehner A (2004) Measuring the navigation multipath channel—a statistical analysis. Proceedings of ION-GNSS-2004, Institute of Navigation, Long Beach, CA, pp 1157–1164

Thevenon P, Julien O, Macabiau C, Serant D, Corazza S, Bousquet M, Ries L, Grelier T (2009) Pseudo-range measurements using OFDM channel estimation. Proceedings of ION-GNSS-2006, Institute of Navigation, Savannah, GA, pp 481–493

Van Dierendonck AJ, Fenton P, Ford T (1992) Theory and performance of narrow correlator spacing in a GPS receiver. Navigation 39(3):265–283

Van Nee RDJ (1993) Spread-spectrum code and carrier synchronization errors caused by multipath and interference. IEEE Trans Aerosp Elecctron Syst 29(4):1359–1365

Wallner S, Hein GW, Pany T, Avila-Rodriguez JA, Posfay A (2005) Interference computations between GPS and Galileo. Proceedings of ION-GNSS-2005, Institute of Navigation, Long Beach, CA, pp 861–876

Zhang J, Lohan ES (2011) Effect of narrowband interference on Galileo E1 signal receiver performance. Int J Navig Obs 2011: 10. Article ID 959871, doi:10.1155/2011/959871

Zou WY, Wu Y (1995) COFDM: an overview. IEEE Trans Broadcast 41(1):1–8

Dr. Xiaoli Liu is an associate professor in the School of Electrical Engineering at Wuhan University, China. She received her M.Sc. in communications and electronics in 1997 from Huazhong University of Science and Techology, China, and her Ph.D in communications and information from Wuhan University in 2007. In 2003, she worked at University of Manitoba as a visiting scholar. She is currently a visiting professor at Miami University, Ohio. Her research activities include signal detection and estimation, modulation schemes for communication and navigation systems, and antenna arrays for high accuracy positioning systems.

Muqing Liang is a Ph.D. candidate at the School of Electrical Engineering, Wuhan University. He received his B.S. in Electrical Engineering from Wuhan University in 2012. His research mainly focuses on modulation schemes for navigation systems.

Dr. Yu Morton is an electrical engineering Professor at Miami University. She received a Ph.D. in electrical engineering from Penn State, MS in EE from Case Western Reserve University, and BS in Physics from Nanjing University. She was a postdoctoral research fellow at the University of Michigan, Space Physics Research Laboratory. Her current research interests are advanced GPS receiver algorithms for accurate and reliable operations in challenging environments, studies of the atmosphere using radar and satellite signals, and development of new applications using satellite navigation technologies. She is the chair of Institute of Navigation Satellite Division and serves on a number of international conference committees, professional society technical committees, and technical publications editorial boards. She is a fellow of IEEE.

Dr. Pau Closas received the M.Sc. and Ph.D. in Electrical Engineering from the Universitat Politècnica de Catalunya (UPC) in 2003 and 2009, respectively. During 2008, he was Research Visitor at the Stony Brook University (SBU), New York, USA. In September 2009, he joined the CTTC, where he currently is a Senior Researcher in the Communications Systems Division and is the Head of the Statistical Inference for Communications and Positioning Department. He has many years of experience in research and industrial projects with both technical and managerial duties. His primary areas of interest include statistical and array signal processing, estimation and detection theory, Bayesian inference, robustness analysis, and game theory with applications to positioning systems, communications systems, and mathematical biology.

Ting Zhang is an assistant software engineer at FiberHome Telecommunication Technologies Co., Ltd. She received her M.Sc. in circuits and systems from Wuhan University in 2013. Her research focuses on baseband signal process for GNSS receivers.

Zhigang Hong received the M.Sc. in photogrammetry and remote sensing from Wuhan University, China in 2006. In 2009, he received a Ph.D. from Wuhan University. He has been a faculty member at the Chinese Academy of Surveying and Mapping (CASM) since 1998, and is the associate deputy director of the key geospatial information engineering laboratory of the National Administration of Surveying, Mapping and Geoinformation. He has many years of experience in research and industrial projects with both technical and managerial duties. His primary research interests include low attitude photogrammetry and satellite mapping.